PHYSICAL REVIEW D **88,** 056002 (2013)

# Semileptonic decays of $B_s$ to $\phi$ meson in QCD

R. Khosravi[1,*] and F. Falahati[2,†]

[1]*Department of Physics, Isfahan University of Technology, Isfahan 84156-83111, Iran*
[2]*Physics Department, Shiraz University, Shiraz 71454, Iran*

(Received 29 June 2013; published 3 September 2013)

The semileptonic $B_s \to \phi\nu\bar{\nu}$, and $B_s \to \phi l^+ l^-$, $l = \tau, \mu, e$ transitions are investigated in the framework of the three-point QCD sum rules in the standard model. These rare decays take place at loop level by electroweak penguin and weak box diagrams in the standard model via the flavor-changing neutral current transition of $b \to s$. Considering the quark condensate contributions, the relevant form factors as well as the branching fractions of these transitions are calculated. The longitudinal lepton polarization and forward-backward asymmetries are also investigated.

DOI: 10.1103/PhysRevD.88.056002 PACS numbers: 11.55.Hx, 13.20.He, 13.75.Lb

## I. INTRODUCTION

Semileptonic $B_s$ meson decays can usually occur through two various processes with different currents. The first group of semileptonic decays can be performed via the weak interaction by the simple tree diagrams. These decays have by far the largest rate in comparison with other decays of the $B_s$ meson [1]. These semileptonic decays allow us to measure the Cabibbo-Kobayashi-Maskawa (CKM) couplings $V_{cb}$ and $V_{ub}$. The second group is the rare semileptonic $B_s$ decays that occur at loop level by electroweak penguin and weak box diagrams in the standard model (SM) via the flavor-changing neutral current (FCNC) transitions of $b \to d$, $s$. Their study is very important in the context of the SM for determination of the CKM matrix elements $V_{tb}$, $V_{td}$, and $V_{ts}$ [2]. On the other hand, the future experimental study of such rare decays can improve the information about $CP$ violation, $T$ violation, and polarization asymmetries in $b \to d$, $s$ penguin channels [3].

The FCNC transitions are dependent on the weak mixing angles of the CKM matrix and can be suppressed also due to their proportionality to small CKM elements [4]. The FCNC decays of the $B_s$ meson are sensitive to new physics contributions to penguin operators. Therefore the benefit of considering these decays is to find the new operators or operators that are subdominant in the SM. Also these decays are extremely interesting for the study of physics beyond the SM, such as the two Higgs doublet model, minimal supersymmetric extension of the SM (MSSM) [5,6], etc.

The $B_s \to \phi l^+ l^-$ decays have been analyzed in some various methods such as lattice QCD [7], light cone QCD sum rules (LCSR) [8], constituent quark model (CQM) [4,9,10], and light front quark model (LFQM) [10–12]. The available experimental measurement of the branching ratio of the exclusive decay of the $B_s \to \phi\mu^+\mu^-$ is given as

$$\mathrm{BR}(B_s \to \phi(1020)\mu^+\mu^-) = (1.23^{+0.40}_{-0.34}) \times 10^{-6}[13]. \quad (1)$$

The $B_s \to \phi\nu\bar{\nu}$ transition is somewhat different. Theoretically, in this decay the photon penguin diagram is absent and there is no hadronic long-distance effects, i.e., charmonium resonances. Experimentally, these modes are very challenging due to the presence of the two neutrinos. Searches for such modes at the $B$ factories use a fully reconstructed $B$ sample or semileptonic tagged mode [1]. The upper limit of the branching ratio for these modes at a 90% confidence level has been reported as follows:

$$\mathrm{BR}(B_s \to \phi(1020)\nu\bar{\nu}) < 5.4 \times 10^{-3}[13]. \quad (2)$$

In this paper, we consider the exclusive $B_s \to \phi l^+ l^- / \nu\bar{\nu}$ decays via the three-point QCD sum rules (3PSR). These decays are related to the transition of $b \to s$ at the quark level as shown in Fig. 1. For analysis of the above-mentioned decays, using the operator product expansion (OPE) in the deep Euclidean region and considering the contributions of the operators with dimensions three, four, and five, we calculate the transition form factors of the semileptonic $B_s \to \phi$ decays. We determine the branching ratios of these FCNC decays and compare these results to the corresponding experimental values and predictions of other methods. Also, we consider the

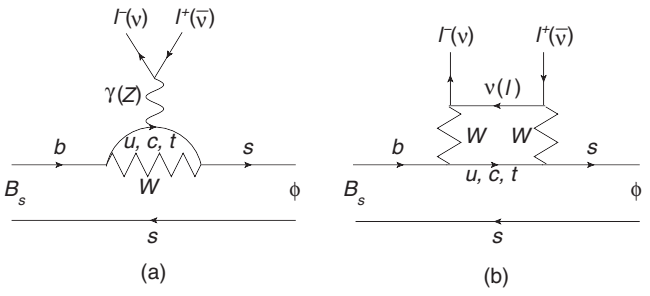


FIG. 1. The loop diagrams of the semileptonic decays of $B_s$ to $\phi$. The electroweak penguin and box diagrams are shown in parts (a) and (b), respectively.

*rezakhosravi@cc.iut.ac.ir
†falahati@shirazu.ac.ir

 

longitudinal lepton polarization asymmetry and forward-backward asymmetry of these semileptonic decays.

The plan of this work is as follows: In Sec. II, we calculate the transition form factors of the $B_s \to \phi$ decay within the three-point QCD sum rules considering the quark-quark and quark-gluon condensate contributions to the correlation function. Also, the calculation of the decay rates for the $B_s \to \phi l^+ l^-$ and $B_s \to \phi \nu \bar{\nu}$ transitions are presented in this section. Section III is devoted to the numeric results and discussions.

## THE FORM FACTORS OF THE $B_s \to \phi$ TRANSITION IN 3PSR

In the SM, the semileptonic $B_s \to \phi l^+ l^-$ and $B_s \to \phi \nu \bar{\nu}$ decays governed by penguin and box diagrams and are not allowed in the tree level. The effective Hamiltonian responsible for these rare decays is described via the $b \to s$ loop transition at the quark level as

$$\mathcal{H}_{\text{eff}} = \frac{G_F \alpha}{2\pi\sqrt{2}} V_{tb} V_{ts}^* \Big[ C_9^{\text{eff}} \bar{s}\gamma_\mu (1-\gamma_5) b \bar{\ell}\gamma_\mu \ell + C_{10} \bar{s}\gamma_\mu (1-\gamma_5) b \bar{\ell}\gamma_\mu \gamma_5 \ell - 2C_7^{\text{eff}} \frac{m_b}{q^2} \bar{s} i\sigma_{\mu\nu} q^\nu (1+\gamma_5) b \bar{\ell}\gamma_\mu \ell \Big], \quad (3)$$

where $C_7^{\text{eff}}$, $C_9^{\text{eff}}$, and $C_{10}$ are the Wilson coefficients, $G_F$ is the Fermi constant, $\alpha$ is the fine structure constant at the $Z$ mass scale, and $V_{ij}$ are the elements of the CKM matrix.

The electromagnetic and Z-penguin and W-box diagrams are shown in Fig. 1. These loop transitions occur via the intermediate $u$, $c$, $t$ quarks. It is important to note that the $b \to s\nu\bar{\nu}$ transition receives contributions only from $Z$-penguin and box diagrams.

The transition amplitude of $B_s \to \phi l^+ l^- / \nu\bar{\nu}$ decays is obtained sandwiching Eq. (3) between the initial and final states, i.e.,

$$\mathcal{M} = \frac{G_F \alpha}{2\pi\sqrt{2}} V_{tb} V_{ts}^* \Big[ C_9^{\text{eff}} \langle \phi(p') \mid \bar{s}\gamma_\mu (1-\gamma_5) b \mid B_s(p) \rangle \times \bar{\ell}\gamma_\mu \ell + C_{10} \langle \phi(p') \mid \bar{s}\gamma_\mu (1-\gamma_5) b \mid B_s(p) \rangle \times \bar{\ell}\gamma_\mu \gamma_5 \ell - 2C_7^{\text{eff}} \frac{m_b}{q^2} \langle \phi(p') \mid \bar{s} i\sigma_{\mu\nu} q^\nu (1+\gamma_5) b \mid \times B_s(p) \rangle \bar{\ell}\gamma_\mu \ell \Big], \quad (4)$$

where $p$ and $p'$ are the momentum of initial and final meson states, respectively. Our main task is to calculate the matrix elements in Eq. (4) involving $J_\mu^A = \bar{s}\gamma_\mu (1-\gamma_5) b$ and $J_\mu^T = \bar{s}\sigma_{\mu\nu} q^\nu (1+\gamma_5) b$, which are the vector–axial vector and tensor–pseudo tensor transition currents, respectively. Using Lorentz invariance and parity conservation, it can be parametrized in terms of some form factors as

$$\begin{aligned}
\langle \phi(p',\epsilon) \mid \bar{s}\gamma_\mu\gamma_5 b \mid B_s(p) \rangle &= \frac{2A_V(q^2)}{m_{B_s}+m_\phi} \varepsilon_{\mu\nu\alpha\beta} \epsilon^{*\nu} p^\alpha p'^\beta, \\
\langle \phi(p',\epsilon) \mid \bar{s}\gamma_\mu b \mid B_s(p) \rangle &= -iA_0(q^2)(m_{B_s}+m_\phi)\epsilon_\mu^* + i\frac{A_1(q^2)}{m_{B_s}+m_\phi}(\epsilon^* p) P_\mu + i\frac{A_2(q^2)}{m_{B_s}+m_\phi}(\epsilon^* p) q_\mu, \\
\langle \phi(p',\epsilon) \mid \bar{s}\sigma_{\mu\nu} q^\nu \gamma_5 b \mid B_s(p) \rangle &= 2T_V(q^2) i\varepsilon_{\mu\nu\alpha\beta} \epsilon^{*\nu} p^\alpha p'^\beta, \\
\langle \phi(p',\epsilon) \mid \bar{s}\sigma_{\mu\nu} q^\nu b \mid B_s(p) \rangle &= T_0(q^2)[\epsilon_\mu^* (m_{B_s}^2 - m_\phi^2) - (\epsilon^* p) P_\mu] + T_1(q^2)(\epsilon^* p)\Big[ q_\mu - \frac{q^2}{m_{B_s}^2 - m_\phi^2} P_\mu \Big],
\end{aligned} \quad (5)$$

where $A_i(q^2)$, $i = V, 0, 1, 2$ and $T_j(q^2)$, $j = V, 0, 1$ are the transition form factors, $P_\mu = (p+p')_\mu$ and $q_\mu = (p-p')_\mu$, and $\epsilon$ is the polarization vector of the $\phi$ meson. Here, $q^2$ is the momentum transfer squared of the $Z$ boson (photon). In order for our calculations to be simple, the following redefinitions of the transition form factors are considered:

$$\begin{aligned}
A_V'(q^2) &= \frac{2A_V(q^2)}{m_{B_s}+m_\phi}, \qquad T_V'(q^2) = -2T_V(q^2), \qquad A_0'(q^2) = A_0(q^2)(m_{B_s}+m_\phi), \qquad T_0'(q^2) = -T_0(q^2)(m_{B_s}^2 - m_\phi^2), \\
A_1'(q^2) &= -\frac{A_1(q^2)}{m_{B_s}+m_\phi}, \qquad T_1'(q^2) = -T_1(q^2), \qquad A_2'(q^2) = -\frac{A_2(q^2)}{m_{B_s}+m_\phi}.
\end{aligned} \quad (6)$$

To calculate the form factors within 3PSR method, we start with the correlation function. The three-correlation function can be constructed from the vacuum expectation value of the time-ordered product of interpolating fields and transition currents $J_\mu^A$ and $J_\mu^T$ as follows,

$$\Pi^A_{\mu\nu}(p^2, p'^2, q^2) = i^2 \int d^4x d^4y e^{-ipx} e^{ip'y} \langle 0 \mid T[J^\phi_\nu(y) J^A_\mu(0) J^{B_s\dagger}(x)] \mid 0\rangle,$$
$$\Pi^T_{\mu\nu}(p^2, p'^2, q^2) = i^2 \int d^4x d^4y e^{-ipx} e^{ip'y} \langle 0 \mid T[J^\phi_\nu(y) J^T_\mu(0) J^{B_s\dagger}(x)] \mid 0\rangle, \tag{7}$$

where $J^\phi_\nu(y) = \bar{s}\gamma_\nu s$ and $J^{B_s}(x) = \bar{s}\gamma_5 b$ are the interpolating currents of the initial and final meson states, respectively. In the QCD sum rules approach, we can obtain the correlation functions of Eq. (7) in two languages—the hadron language, which is the physical or phenomenological side, and the quark gluon language called the QCD or theoretical side. Equating two sides and applying the double Borel transformations with respect to the momentum of the initial and final states to suppress the contribution of the higher states and continuum, we get sum rule expressions for our form factors. To drive the phenomenological part, two complete sets of intermediate states with the same quantum numbers as the currents $J^\phi$ and $J^{B_s}$ are inserted. As a result of this procedure,

$$\Pi^A_{\mu\nu}(p^2, p'^2, q^2) = -\frac{\langle 0 \mid J^\phi_\nu \mid \phi(p', \varepsilon)\rangle \langle \phi(p', \varepsilon) \mid J^A_\mu \mid B_s(p)\rangle \langle B_s(p) \mid J^{B_s\dagger} \mid 0\rangle}{(p'^2 - m^2_\phi)(p^2 - m^2_{B_s})}$$
$$+ \text{higher resonances and continuum states},$$
$$\Pi^T_{\mu\nu}(p^2, p'^2, q^2) = -\frac{\langle 0 \mid J^\phi_\nu \mid \phi(p', \varepsilon)\rangle \langle \phi(p', \varepsilon) \mid J^T_\mu \mid B_s(p)\rangle \langle B_s(p) \mid J^{B_s\dagger} \mid 0\rangle}{(p'^2 - m^2_\phi)(p^2 - m^2_{B_s})}$$
$$+ \text{higher resonances and continuum states}. \tag{8}$$

The following matrix elements are defined in the standard way in terms of the leptonic decay constants of $\phi$ and $B_s$ mesons as

$$\langle 0 \mid J^\phi_\nu \mid \phi(p', \epsilon)\rangle = f_\phi m_\phi \epsilon_\nu,$$
$$\langle 0 \mid J^{B_s} \mid B_s(p)\rangle = -i\frac{f_{B_s} m^2_{B_s}}{m_b + m_s}. \tag{9}$$

Using Eq. (5), (6), and (9) in Eq. (8) and performing summation over the polarization of the $\phi$ meson, we obtain

$$\Pi^A_{\mu\nu}(p^2, p'^2, q^2) = -\frac{f_{B_s} m^2_{B_s}}{(m_b + m_s)} \frac{f_\phi m_\phi}{(p'^2 - m^2_\phi)(p^2 - m^2_{B_s})}$$
$$\times [iA'_V(q^2)\varepsilon_{\mu\nu\alpha\beta} p^\alpha p'^\beta + A'_0(q^2) g_{\mu\nu}$$
$$+ A'_1(q^2) P_\mu p_\nu + A'_2(q^2) q_\mu p_\nu]$$
$$+ \text{excited states},$$
$$\Pi^T_{\mu\nu}(p^2, p'^2, q^2) = -\frac{f_{B_s} m^2_{B_s}}{(m_b + m_s)} \frac{f_\phi m_\phi}{(p'^2 - m^2_\phi)(p^2 - m^2_{B_s})}$$
$$\times [T'_V(q^2)\varepsilon_{\mu\nu\alpha\beta} p^\alpha p'^\beta - iT'_0(q^2) g_{\mu\nu}$$
$$- iT'_1(q^2) q_\mu p_\nu] + \text{excited states}. \tag{10}$$

To calculate the form factors $A'_i$ and $T'_j$, we will choose the structures $i\varepsilon_{\mu\nu\alpha\beta} p^\alpha p'^\beta$, $g_{\mu\nu}$, $P_\mu p_\nu$, $q_\mu p_\nu$, from $\Pi^A_{\mu\nu}$ and $\varepsilon_{\mu\nu\alpha\beta} p^\alpha p'^\beta$, $ig_{\mu\nu}$ and $iq_\mu p_\nu$ from $\Pi^T_{\mu\nu}$, respectively.

On the QCD side, using the OPE, we can obtain the correlation functions in quark gluon language in the deep Euclidean region where $p^2 \ll (m_b + m_s)^2$ and $p'^2 \ll 4m_s^2$. For this aim, the correlations are written as

$$\Pi^A_{\mu\nu}(p^2, p'^2, q^2) = i\Pi^A_V \varepsilon_{\mu\nu\alpha\beta} p^\alpha p'^\beta + \Pi^A_0 g_{\mu\nu}$$
$$+ \Pi^A_1 P_\mu p_\nu + \Pi^A_2 q_\mu p_\nu,$$
$$\Pi^T_{\mu\nu}(p^2, p'^2, q^2) = \Pi^T_V \varepsilon_{\mu\nu\alpha\beta} p^\alpha p'^\beta - i\Pi^T_0 g_{\mu\nu}$$
$$- i\Pi^T_1 q_\mu p_\nu, \tag{11}$$

where, each $\Pi^A_i$ and $\Pi^T_j$ function is defined in terms of the perturbative and nonperturbative parts as

$$\Pi^{A,T}(p^2, p'^2, q^2) = \Pi^{A,T}_{\text{per}}(p^2, p'^2, q^2)$$
$$+ \Pi^{A,T}_{\text{nonper}}(p^2, p'^2, q^2). \tag{12}$$

For the perturbative part, the bare loop diagrams in Fig. 1 are considered. With the help of the double dispersion representation, the bare-loop contribution is written as

$$\Pi^{A,T}_{\text{per}} = -\frac{1}{(2\pi)^2} \int ds' \int ds \frac{\rho^{A,T}(s, s', q^2)}{(s - p^2)(s' - p'^2)}$$
$$+ \text{subtraction terms}. \tag{13}$$

The spectral densities $\rho^{A,T}(s, s', q^2)$ are calculated by the help of the Gutkosky rules, i.e., the propagators are replaced by Dirac delta functions $\frac{1}{p^2 - m^2} \to -2\pi i\delta(p^2 - m^2)$ expressing that all quarks are real.

Straightforward calculations end up in the following results for the spectral densities related to $j^A_\mu$ and $j^T_\mu$ vertices:

$$\rho_0^A = -2N_c I_0[(4D_1 + s')(m_s - m_b) - m_s u],$$
$$\rho_V^A = -4N_c I_0[m_s - B_1(m_b - m_s)],$$
$$\rho_1^A = -2N_c I_0[2(D_2 + D_3)(m_b - m_s) + B_1(m_b - 3m_s) - m_s],$$
$$\rho_2^A = -2N_c I_0[4(D_2 - D_3)(m_b - m_s) - 2B_1(m_b + m_s) + 2m_s],$$
$$\rho_0^T = -2N_c I_0[s'(\Delta - s) + m_s(m_b - m_s)(2s' - u) - D_1(4s - 2u)],$$
$$\rho_V^T = -4N_c I_0[B_1(\Delta - s) + m_s(m_b + m_s)],$$
$$\rho_1^T = -2N_c I_0[(D_2 - D_3)(2s - u) + B_1(\Delta - s' - s) + B_2 s' + (m_b - m_s)m_s],$$

where

$$I_0(s, s', q^2) = \frac{1}{2\lambda^{1/2}(s, s', q^2)},$$
$$\lambda(a, b, c) = a^2 + b^2 + c^2 - 2ac - 2bc - 2ab,$$
$$\Delta = (s + m_s^2 - m_b^2),$$
$$u = s + s' - q^2,$$
$$B_1 = \frac{1}{\lambda(s, s', q^2)}[2s'\Delta - s'u],$$
$$B_2 = \frac{1}{\lambda(s, s', q^2)}[2ss' - \Delta u],$$
$$D_1 = -\frac{1}{2\lambda(s, s', q^2)}[(4ss'm_s^2 - ss'^2 - s'\Delta^2 - u^2 m_s^2 + u\Delta s')],$$
$$D_2 = -\frac{1}{\lambda^2(s, s', q^2)}[8ss'^2 m_s^2 - 2ss'^3 - 6s'^2\Delta^2 - 2u^2 s' m_s^2 + 6s'^2 u\Delta - u^2 s'^2],$$
$$D_3 = \frac{1}{\lambda^2(s, s', q^2)}[4ss'um_s^2 + 4ss'^2\Delta - 3ss'^2 u - 3u\Delta^2 s' - u^3 m_s^2 + 2u^2\Delta s'],$$

and $N_c = 3$ is the color factor.

The physical region in the $s$ and $s'$ plane is described by the following inequalities:

$$-1 \le \frac{2s(s' + 1) - \Delta(s + s' - q^2)}{\lambda^{1/2}(m_b^2, s, m_s^2)\lambda^{1/2}(s, s', q^2)} \le +1, \quad (14)$$

and from this inequality, to use in the lower limit of the integration over $s$ in Eq. (13), it is easy to express $s$ in terms of $s0$, i.e., $sL$ is as follows:

$$s_L = \frac{(m_s^2 + q^2 - m_b^2 - s')(m_b^2 s' - q^2 m_s^2)}{(m_b^2 - q^2)(m_s^2 - s')}. \quad (15)$$

Now, the nonperturbative contributions to the correlation function are discussed [Eq. (12)]. In QCD, the three-point correlation function can be evaluated by the OPE in the deep Euclidean region. Using the expansion of the nonperturbative part in terms of a series of local operators with increasing dimension, we get [13,14]

$$\Pi_{\text{nonper}}^{A,T}(p^2, p'^2, q^2) = C_3^{A,T}\langle\bar{\Psi}\Psi\rangle + C_4^{A,T}\langle G^2\rangle + C_5^{A,T}\langle\bar{\Psi}\sigma_{\alpha\beta}T^a G^{a\alpha\beta}\Psi\rangle + C_6^{A,T}\langle\bar{\Psi}\Gamma\Psi\bar{\Psi}\Gamma'\Psi\rangle + \cdots, \quad (16)$$

where $C_k^{A,T}$ are the Wilson coefficients, $\Psi$ is the local fermion field operator of quarks, $G_{\alpha\beta}$ is the gluon field strength tensor, and $\Gamma$ and $\Gamma'$ are the matrices appearing in the calculations.

In Eq. (16) the condensate terms of dimensions three and five are related to contributions of quark-quark and quark-gluon condensate, respectively. It's found that the heavy quark condensate contributions are exponentially suppressed by heavy quark masses [13]. Our calculations show that in this case, the gluon-gluon condensate contributions of dimension four are very small in comparison with the quark condensate contributions of dimension three and five so that we can easily ignore their contributions in our calculations. Therefore, only three important diagrams remain from the nonperturbative part contributions. The diagrams of the effective contributions of the condensate terms are depicted in Fig. 2.

The next step is to apply the Borel transformations with respect to the $p^2(p^2 \to M_1^2)$ and $p'^2(p'^2 \to M_2^2)$ on the phenomenological as well as the perturbative and nonperturbative parts of the correlation functions and equate these two representations of the correlations. The following sum rules for the form factors are derived:

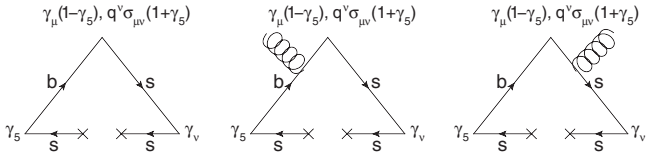


FIG. 2. Nonperturbative diagrams for the semileptonic decays of $B_s \to \phi$.

$$
\begin{aligned}
A_i'(q^2) &= \frac{(m_b+m_s)}{f_{B_s} m_{B_s}^2 f_\phi m_\phi} e^{m_{B_s}^2/M_1^2} e^{m_\phi^2/M_2^2} \\
&\times \left\{ -\frac{1}{4\pi^2} \int_{(2m_s)^2}^{s_0'} ds' \int_{s_L}^{s_0} ds \rho_i^A(s,s',q^2) e^{-s/M_1^2} \right. \\
&\left. \times e^{-s'/M_2^2} + M_1^2 M_2^2 \frac{\langle s\bar{s}\rangle}{24} C_i^A(p^2,p'^2,q^2) \right\}, \\
T_j'(q^2) &= \frac{(m_b+m_s)}{f_{B_s} m_{B_s}^2 f_\phi m_\phi} e^{m_{B_s}^2/M_1^2} e^{m_\phi^2/M_2^2} \\
&\times \left\{ -\frac{1}{4\pi^2} \int_{(2m_s)^2}^{s_0'} ds' \int_{s_L}^{s_0} ds \rho_j^T(s,s',q^2) \right. \\
&\left. \times e^{-s/M_1^2} e^{-s'/M_2^2} + M_1^2 M_2^2 \frac{\langle s\bar{s}\rangle}{24} C_j^T(p^2,p'^2,q^2) \right\},
\end{aligned}
\tag{17}
$$

where $s_0$ and $s_0'$ are the continuum thresholds and $s_L$ is the lower limit of the integral over $s$ presented in Eq. (15).

The explicit expressions of the $C_i^A$ and $C_j^T$ of the quark condensate coefficients with dimensions three and five are given in the Appendix.

In our calculation, the following Borel transformations are also used:

$$
\begin{aligned}
\mathcal{B}_{p^2}(M_1^2)\left(\frac{1}{p^2-m_b^2}\right)^m &= \frac{(-1)^m}{\Gamma(m)} \frac{e^{-\frac{m_b^2}{M_1^2}}}{(M_1^2)^m}, \\
\mathcal{B}_{p'^2}(M_2^2)\left(\frac{1}{p'^2-m_s^2}\right)^n &= \frac{(-1)^n}{\Gamma(n)} \frac{e^{-\frac{m_s^2}{M_2^2}}}{(M_2^2)^n}.
\end{aligned}
\tag{18}
$$

At the end of this section, we present the dilepton invariant mass distribution for the $B_s \to \phi \nu \bar{\nu}$ and $B_s \to \phi l^+ l^-$ decays. Using the parametrization of the $B_s \to \phi$ transition in terms of form factors and also Eq. (4), the dilepton invariant mass distribution of the $B_s \to \phi \nu \bar{\nu}$ decay can be written as [10]

$$
\frac{d\Gamma(B_s \to \phi \nu \bar{\nu})}{ds} = \frac{G_F^2 |V_{tb} V_{ts}^*|^2 \alpha^2 |D(x_t)|^2 m_{B_s}^5}{2^8 \pi^5 \sin^4\theta_W} \lambda_\phi^{1/2} H_\phi,
\tag{19}
$$

where $s = q^2/m_{B_s}^2$ and $x_t = m_t^2/m_W^2$. The parameters $D(x_t)$, $\lambda_\phi$ and $H_\phi$ are defined by

$$
\begin{aligned}
D(x_t) &= \frac{x_t}{8}\left(\frac{2+x_t}{x_t-1} + \frac{3x_t-6}{(x_t-1)^2}\ln x_t\right), \qquad \lambda_\phi = (1-r_\phi)^2 - 2s(1+r_\phi) + s^2, \\
H_\phi &= 3s\left[(1-\sqrt{r}_\phi)^2 |A_0|^2 + \frac{\lambda_\phi}{(1+\sqrt{r}_\phi)^2}|A_V|^2\right] + \lambda_\phi\left[\frac{(1-\sqrt{r}_\phi)^2}{4r_\phi}|A_0|^2 - \frac{s}{(1+\sqrt{r}_\phi)^2}|A_V|^2\right. \\
&\left. + \frac{\lambda_\phi}{4r_\phi(1+\sqrt{r}_\phi)^2}|A_1|^2 + \frac{(1-r_\phi-s)(1-\sqrt{r}_\phi)}{2r_\phi(1+\sqrt{r}_\phi)}\mathrm{Re}(A_0 A_1^*)\right],
\end{aligned}
\tag{20}
$$

where $r_\phi = m_\phi^2/m_{B_s}^2$. The differential decay rates for $B_s \to \phi l^+ l^-$ are found to be [10]

$$
\frac{d\Gamma(B_s \to \phi l^+ l^-)}{ds} = \frac{G_F^2 |V_{tb} V_{ts}^*|^2 m_{B_s}^5 \alpha^2}{3 \times 2^9 \pi^5}\left(1-\frac{4\hat{l}}{s}\right)^{\frac{1}{2}} \lambda_\phi^{1/2}\left[\left(1+\frac{2\hat{l}}{s}\right)\alpha_\phi + t\delta_\phi\right],
\tag{21}
$$

where $\hat{l} = m_l^2/m_{B_s}^2$. The formulas of $\alpha_\phi$ and $\delta_\phi$ are given by

$$
\begin{aligned}
\alpha_\phi &= 4s[3(1-r_\phi)^2(|G_0|^2+|F_0|^2) + 2\lambda_\phi(|G_V|^2+|F_V|^2)] + \frac{\lambda_\phi}{r_\phi}[(1-r_\phi)^2(|G_0|^2+|F_0|^2) + \lambda_\phi(|G_1|^2+|F_1|^2) \\
&+ 2(1-r_\phi)(1-r_\phi-s)\,\mathrm{Re}(G_0 G_1^* + F_0 F_1^*)], \\
\delta_\phi &= -48\lambda_\phi |F_V|^2 - 72(1-r_\phi)^2|F_0|^2 + \frac{6[2(1+r_\phi)-s]}{r_\phi}\lambda_\phi |F_1|^2 + \frac{6s}{r_\phi}\lambda_\phi |F_2|^2 + \frac{12(1-r_\phi)}{r_\phi}\lambda_\phi \\
&\times \mathrm{Re}(F_0 F_1^* + F_0 F_2^* + F_1 F_2^*),
\end{aligned}
\tag{22}
$$

where the functions $G_V$, $F_V$, $G_0$, $F_0$, $G_1$, $F_1$, and $F_2$ are defined by

$$
\begin{aligned}
G_V &= \frac{C_9^{\rm eff} A_V}{2(1+\sqrt{r_\phi})} - \frac{C_7^{\rm eff}\hat{m}_b T_V}{s}, \\
F_V &= \frac{C_{10} A_V}{2(1+\sqrt{r_\phi})}, \\
G_0 &= \frac{C_9^{\rm eff} A_0}{2(1+\sqrt{r_\phi})} - \frac{C_7^{\rm eff}\hat{m}_b T_0}{s}, \\
F_0 &= \frac{C_{10} A_0}{2(1+\sqrt{r_\phi})}, \\
G_1 &= \frac{C_9^{\rm eff} A_1}{2(1+\sqrt{r_\phi})} - \frac{C_7^{\rm eff}\hat{m}_b T_1}{s}, \\
F_1 &= \frac{C_{10} A_1}{2(1+\sqrt{r_\phi})}, \\
F_2 &= \frac{C_{10} A_2}{2(1+\sqrt{r_\phi})},
\end{aligned}
\tag{23}
$$

with $\hat{m}_b = m_b/m_{B_s}$.

## III. NUMERICAL ANALYSIS

In this section, we present our numerical analysis of the form factors $A_i$ ($i = V, 0, 1, 2$) and $T_j$ ($j = V, 0, 1$). From the sum rules expressions of the form factors, it is clear that the main input parameters entering the expressions are quark condensates, Wilson coefficients $C_7^{\rm eff}$, $C_9^{\rm eff}$, and $C_{10}$, elements of the CKM matrix $V_{tb}$ and $V_{ts}$, leptonic decay constants $f_{B_s}$ and $f_\phi$, Borel parameters $M_1^2$ and $M_2^2$, as well as the continuum thresholds $s_0$ and $s_0'$. We choose the values of quark, lepton, and meson masses as $m_s = 0.150$ GeV ($\mu = 1$ GeV) [15], $m_b = 4.8$ GeV [16], $m_\mu = 0.105$ GeV, $m_\tau = 1.776$ GeV, $m_\phi = 1.019$ GeV, $m_{B_s} = 5.366$ GeV [17]. We also choose the values of the condensates (at a fixed renormalization scale of about 1 GeV), Wilson coefficients, leptonic decay constants, and CKM matrix elements as shown in Table I.

The sum rules for the form factors also contain four auxiliary parameters, namely Borel mass squares, $M_1^2$ and $M_2^2$, and continuum thresholds, $s_0$ and $s_0'$. These are not physical quantities, so our results should be independent of them. The parameters $s_0$ and $s_0'$ are not totally arbitrary, but they are related to the energy of the first excited states with the same quantum numbers as the interpolating currents. They are determined from the conditions that guarantee the sum rules to have the best stability in the allowed $M_1^2$ and $M_2^2$ regions. The values of continuum thresholds $s_0$ and $s_0'$ calculated from the two-point QCD sum rules are taken to be $s_0 = (35.4 \pm 0.5)$ GeV$^2$ [18] and $s_0' = (2.0 \pm 0.1)$ GeV$^2$ [20]. The working regions for $M_1^2$ and $M_2^2$ are determined demanding not only that the contributions of the higher states and continuum are effectively suppressed but also that the contributions of the higher-dimensional operators are small. Both conditions are satisfied in the regions, 12 GeV$^2 \leq M_1^2 \leq 20$ GeV$^2$ and 4 GeV$^2 \leq M_2^2 \leq 10$ GeV$^2$.

Figure 3 shows a good stability of the form factors with respect to the Borel mass parameters in the working regions. Using these regions for $M_1^2$ and $M_2^2$, our numerical analysis shows that the contribution of the nonperturbative part to the QCD side is about 21% of the total, and the main contribution comes from the perturbative part.

Now, we proceed to present the $q^2$ dependency of the form factors. Since the form factors $A_i(q^2)$ and $T_j(q^2)$ are calculated in the spacelike ($q^2 < 0$) region, we should analytically continue them to the timelike ($q^2 > 0$), or physical, region. Therefore, to extend our results to the full physical region, we look for parametrization of the form factors in such a way that in the reliable region the results of the parametrization coincide with the sum rules predictions. Our numerical calculation shows that the sufficient parametrization of the form factors with respect to $q^2$ is

$$
f_i(q^2) = \frac{f_i(0)}{1 - \alpha s + \beta s^2}. \tag{24}
$$

We evaluated the values of the parameters $f_i(0)$, $\alpha$, and $\beta$ for each transition form factor of the $B_s \to \phi$ decay, taking $M_1^2 = 15$ GeV$^2$ and $M_2^2 = 8$ GeV$^2$. Table II shows the values of the form factors $A_i$ and $T_j$ at $q^2 = 0$. Also, this table contains the predictions of the light-cone QCD sum rules (LCSR), the light front quark model (LFQM), and the constituent quark model (CQM).

The values of the parameters $\alpha$ and $\beta$ for each form factor of the $B_s \to \phi$ transition are presented in Table III.

TABLE I. Input values in numerical calculations.

| Input Parameters | Values | Ref. | Input Parameters | Values | Ref. |
|---|---|---|---|---|---|
| $m_W$ | $80.385 \pm 0.015$ GeV | [17] | $f_\phi$ | $0.231 \pm 0.004$ GeV | [18] |
| $\sin^2\theta_W$ | 0.2314 | [17] | $f_{B_s}$ | $0.183 \pm 0.014$ GeV | [18] |
| $G_F$ | $1.16637 \times 10^{-5}$ GeV$^{-2}$ | [17] | $\mid V_{tb}V_{ts}^* \mid$ | 0.0385 | [19] |
| $m_t$ | $175.5 \pm 4.1$ GeV | [17] | $C_7^{\rm eff}$ | $-0.313$ | [19] |
| $m_0^2$ | $0.8 \pm 0.2$ GeV$^2$ | [13] | $C_9$ | 4.344 | [19] |
| $\langle u\bar{u}\rangle$ | $-(0.240 \pm 0.010)^3$ GeV$^3$ | [13] | $C_{10}$ | $-4.669$ | [19] |
| $\langle s\bar{s}\rangle$ | $(0.8 \pm 0.2)\langle u\bar{u}\rangle$ GeV$^3$ | [13] | | | |

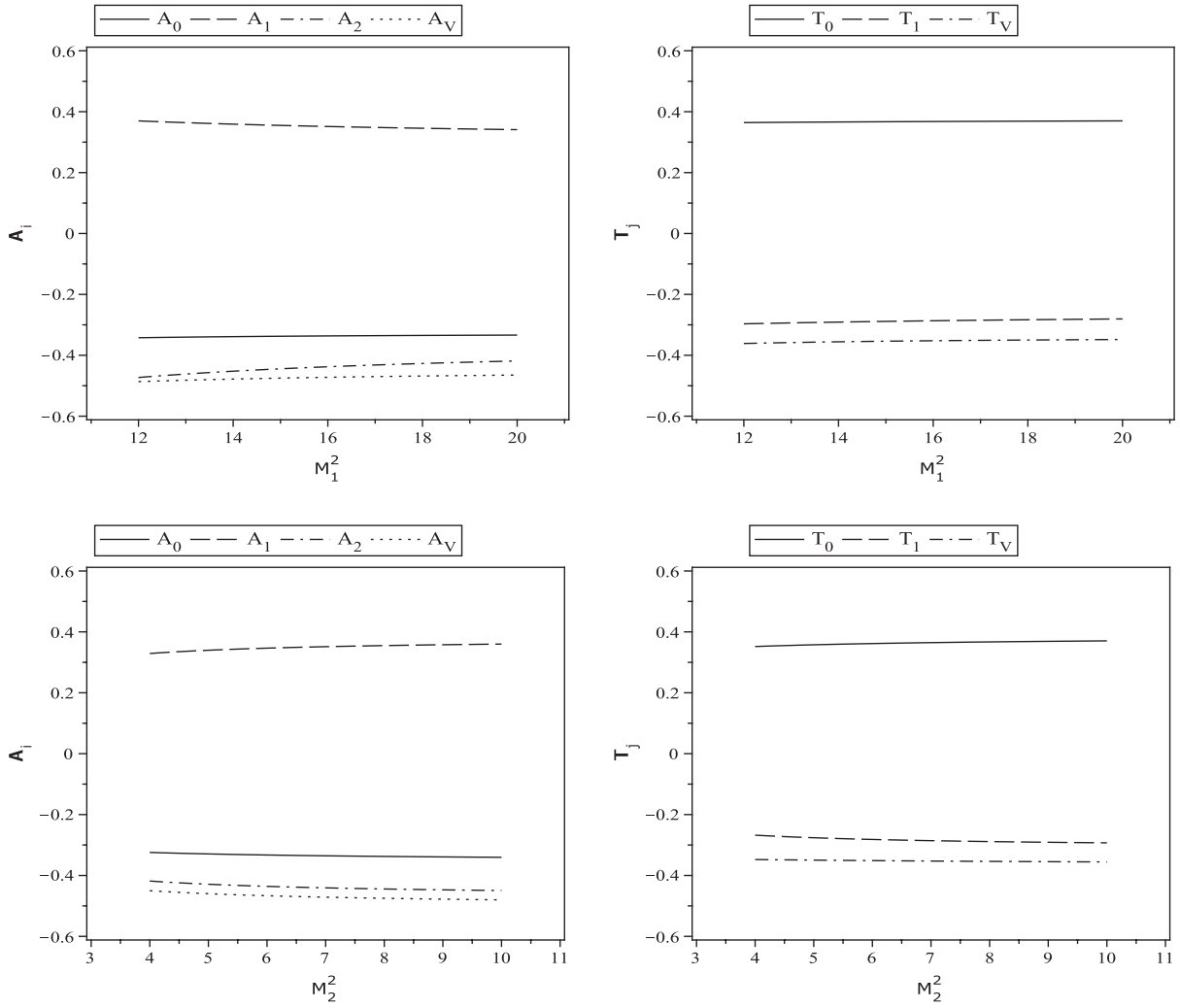


FIG. 3. The form factors $A_i$ and $T_j$ on $M_1^2$ and $M_2^2$.

The dependence of the form factors $A_i(q^2)$ and $T_j(q^2)$ on $q^2$ extracted from the fit function is given in Fig. 4.

Now we would like to evaluate the branching ratios for the considered decays. Using Eqs. (19)–(21) and integrating them over $q^2$ in the whole physical region and using the total mean lifetime $\tau_{B_s} = (1.497 \pm 0.015)$ ps [17], the branching ratios of the $B_s \to \phi l^+ l^-/\nu\bar{\nu}$ are obtained as presented in Table IV. This table also includes a comparison between

TABLE II. The values of the $A_i(0)$ and $T_j(0)$ in comparison with the predictions of the other nonperturbative approaches, such as LCSR, CQM, and LFQM.

| Models | $A_0(0)$ | $A_1(0)$ | $A_2(0)$ | $A_V(0)$ | $T_0(0)$ | $T_1(0)$ | $T_V(0)$ |
|---|---|---|---|---|---|---|---|
| This Work (3PSR) | −0.34 | 0.35 | −0.44 | −0.47 | 0.37 | −0.28 | −0.35 |
| LCSR [8] | 0.30 | 0.26 | 0.38 | 0.43 | 0.35 | 0.35 | 0.25 |
| CQM [9] | 0.34 | 0.31 | 0.42 | 0.44 | 0.38 | 0.38 | 0.26 |
| CQM [10] | −0.506 | 0.310 | −0.379 | −0.445 | 0.380 | −0.380 | 0.380 |
| LFQM [10] | −0.464 | 0.276 | −0.295 | −0.440 | 0.374 | −0.374 | 0.377 |

TABLE III. The values of the parameter $\alpha$ and $\beta$ for each form factor.

| Parameters | $A_0(q^2)$ | $A_1(q^2)$ | $A_2(q^2)$ | $A_V(q^2)$ | $T_0(q^2)$ | $T_1(q^2)$ | $T_V(q^2)$ |
|---|---|---|---|---|---|---|---|
| $\alpha$ | 0.27 | 0.92 | 0.99 | 1.29 | 0.33 | 1.05 | 1.29 |
| $\beta$ | −1.16 | 0.26 | 0.11 | 0.16 | −0.02 | 0.24 | 0.12 |

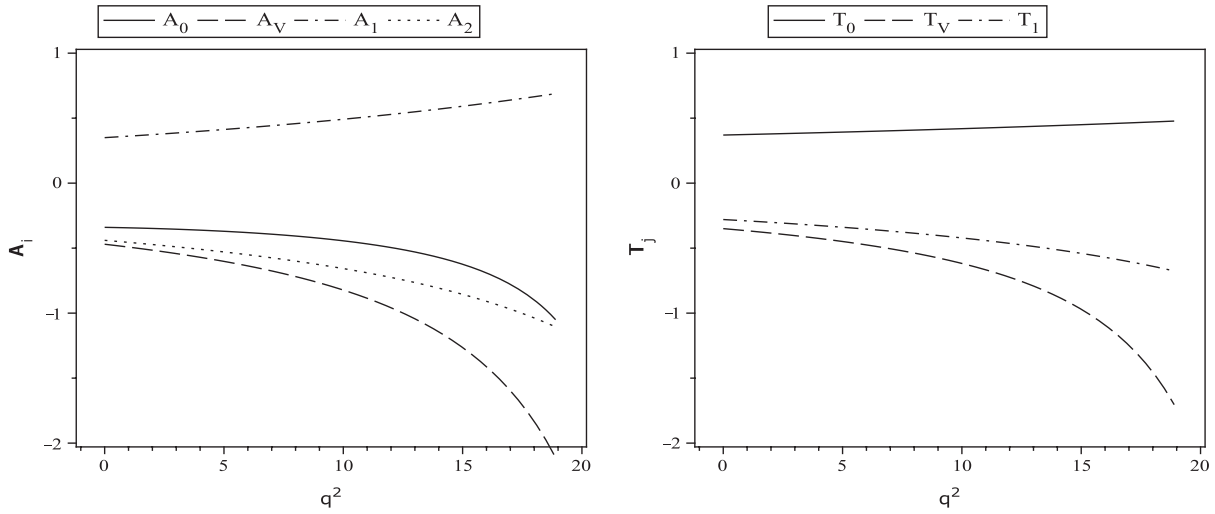


FIG. 4. The form factors $A_i$ and $T_j$ on $q^2$.

our results and predictions of the other approaches in the SM, including the LFQM, CQM, and LCSR approaches. From Table IV, we see a good consistency in order of magnitude between our results and predictions of the other nonperturbative approaches.

So far, the transition form factors and branching ratio values were investigated via the $SU_f(3)$ symmetry breaking, and the mass of the $s$ quark was considered in the expressions of the condensate terms and spectral densities. Now we want to analyze the form factors, considering the $SU_f(3)$ symmetry. For the stated purpose, the mass of the $s$ quark is ignored in all equations, i.e., $m_s \to m_u \simeq 0$ GeV and $\langle s\bar{s}\rangle \to \langle u\bar{u}\rangle$. In view of the $SU_f(3)$ symmetry, the values of the branching ratios of the $B_s \to \phi l^+ l^-$ are shown in Table V.

In Table IV, we show only the values obtained considering the short-distance (SD) effects contributing to the

TABLE IV. The branching ratios of the semileptonic $B_s \to \phi$ transition in different models.

| Mode | This work | LFQM [10] | CQM [10] | LCSR [6] | CQM [6] | CQM [4] |
|---|---|---|---|---|---|---|
| $\mathrm{Br}(B_s \to \phi\nu\bar{\nu}) \times 10^6$ | $6.59 \pm 1.98$ | 12.02 | 11.65 | ⋯ | ⋯ | ⋯ |
| $\mathrm{Br}(B_s \to \phi e^+ e^-) \times 10^6$ | $2.95 \pm 0.89$ | 1.72 | 1.69 | 2.01 | 1.87 | ⋯ |
| $\mathrm{Br}(B_s \to \phi \mu^+ \mu^-) \times 10^6$ | $2.52 \pm 0.76$ | 1.64 | 1.61 | 1.65 | 1.25 | 2.5 |
| $\mathrm{Br}(B_s \to \phi \tau^+ \tau^-) \times 10^7$ | $1.20 \pm 0.36$ | 1.60 | 1.51 | 1.38 | 2.28 | ⋯ |

TABLE V. The branching ratios of the semileptonic $B_s \to \phi l^+ l^-$ decays considering $SU_f(3)$ symmetry.

| Mode | Value |
|---|---|
| $\mathrm{Br}(B_s \to \phi\nu\bar{\nu}) \times 10^6$ | $3.58 \pm 2.22$ |
| $\mathrm{Br}(B_s \to \phi e^+ e^-) \times 10^6$ | $1.96 \pm 0.64$ |
| $\mathrm{Br}(B_s \to \phi \mu^+ \mu^-) \times 10^6$ | $1.63 \pm 0.53$ |
| $\mathrm{Br}(B_s \to \phi \tau^+ \tau^-) \times 10^7$ | $0.72 \pm 0.23$ |

TABLE VI. The branching ratios of the semileptonic $B_s \to \phi l^+ l^-$ decays including LD effects in three regions.

| Mode | Method | I | II | III | I + II + III | EXP [17] |
|---|---|---|---|---|---|---|
| $\mathrm{Br}(B_s \to \phi \mu^+ \mu^-) \times 10^7$ | This work | $8.93 \pm 2.98$ | $1.39 \pm 0.42$ | $2.29 \pm 0.69$ | $12.6 \pm 4.9$ | $12.3^{+4.0}_{-3.4}$ |
| | LFQM [10] | 7.91 | 1.88 | 2.56 | 12.4 | |
| | CQM [10] | 8.30 | 1.83 | 2.23 | 12.4 | |
| | CQM [4] | ⋯ | ⋯ | ⋯ | 19.0 | |
| $\mathrm{Br}(B_s \to \phi \tau^+ \tau^-) \times 10^8$ | This work | ⋯ | $0.13 \pm 0.04$ | $8.46 \pm 2.54$ | $8.59 \pm 2.92$ | ⋯ |
| | LFQM [10] | ⋯ | 0.48 | 8.87 | 9.35 | |
| | CQM [10] | ⋯ | 0.48 | 8.31 | 8.79 | |

Wilson coefficient $C_9^{\rm eff}$ for the charged lepton case. In this part, we would like to present the branching ratios including long-distance (LD) effects. The effective Wilson coefficient $C_9^{\rm eff}$ including both the SD and LD effects is [21]

$$C_9^{\rm eff}(s) = C_9 + C_9^{\rm SD}(s) + C_9^{\rm LD}(s). \tag{25}$$

The LD effect contributions are due to the $J/\psi$ family. The explicit expressions of the $C_9^{\rm SD}(s)$ and $C_9^{\rm LD}(s)$ can be found in [21] (see also [19]). We introduce some cuts around the resonances of $J/\psi$ and $\psi'$ and study the following three regions for muon:

$$\begin{aligned} &\text{I: } \sqrt{q^2_{\rm min}} \le \sqrt{q^2} \le M_{J/\psi} - 0.20, \\ &\text{II: } M_{J/\psi} + 0.04 \le \sqrt{q^2} \le M_{\psi'} - 0.10, \\ &\text{III: } M_{\psi'} + 0.02 \le \sqrt{q^2} \le m_{B_s} - m_\phi \end{aligned} \tag{26}$$

and the following two for tau:

$$\begin{aligned} &\text{I: } \sqrt{q^2_{\rm min}} \le \sqrt{q^2} \le M_{\psi'} - 0.02, \\ &\text{II: } M_{\psi'} + 0.02 \le \sqrt{q^2} \le m_{B_s} - m_\phi, \end{aligned} \tag{27}$$

where $\sqrt{q^2_{\rm min}} = 2m_l$. In Table VI we present the branching ratios for muon and tau obtained using the regions shown in Eqs. (26) and (27), respectively. In other words, we present the branching ratios using the complete expression of Eq. (21) but exclude the $c\bar{c}$ resonance regions. Here, we should also stress that the results obtained for the electron are very close to the results of the muon, and for this reason, we only present the branching ratios for the muon in our table. It is interesting to point out that the values of $\mathrm{Br}(B_s \to \phi\mu^+\mu^-)$ in this work and in the LFQM [10] and CQM [10] are close to the experimental data.

We also show the dependency of the differential branching ratios on $q^2$ (with and without LD effects for the charged lepton case) in Fig. 5.

Finally, we want to calculate the longitudinal lepton polarization asymmetry and the forward-backward

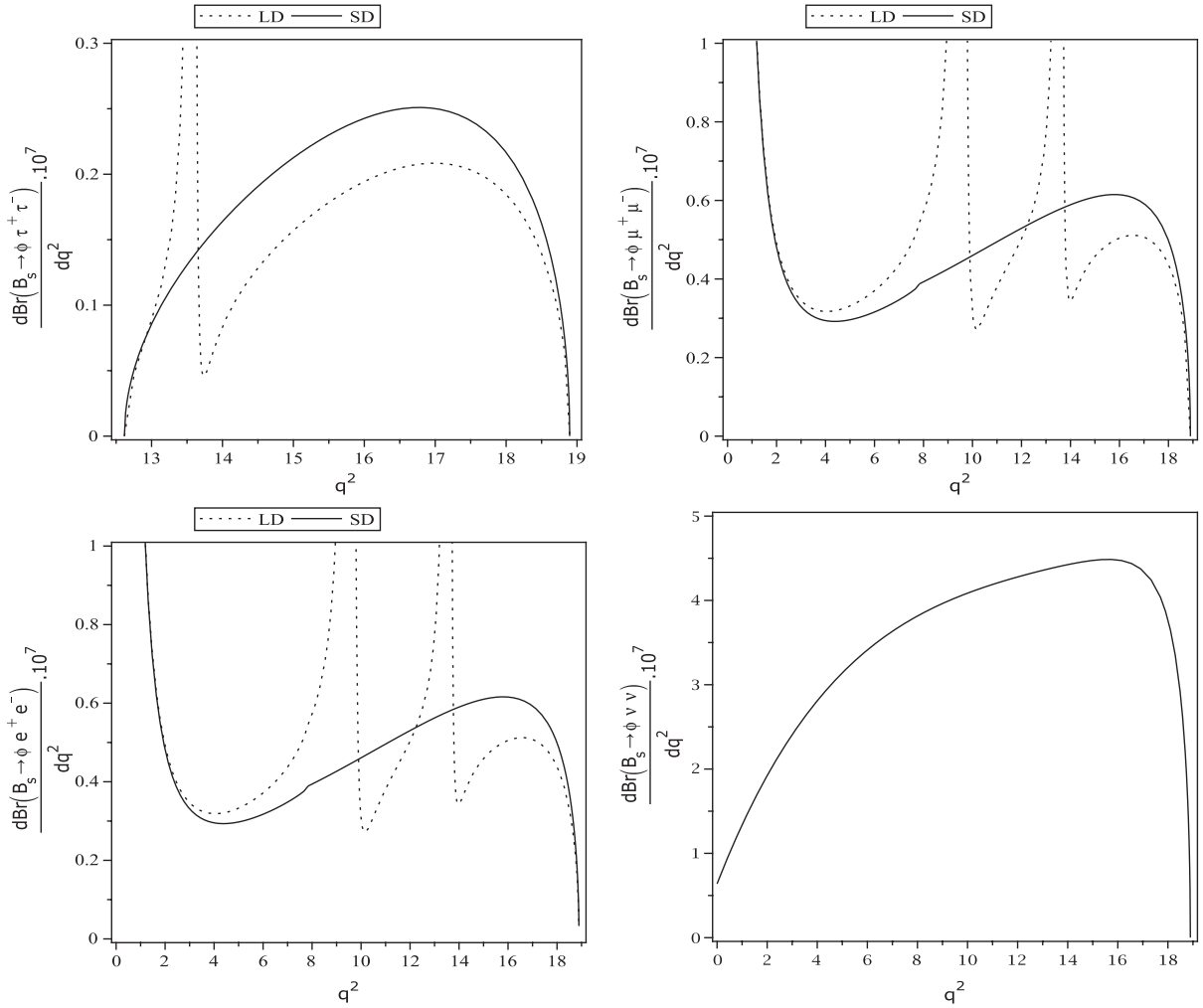


FIG. 5. The differential branching ratios of semileptonic $B_s \to \phi$ decays on $q^2$ with and without LD effects.

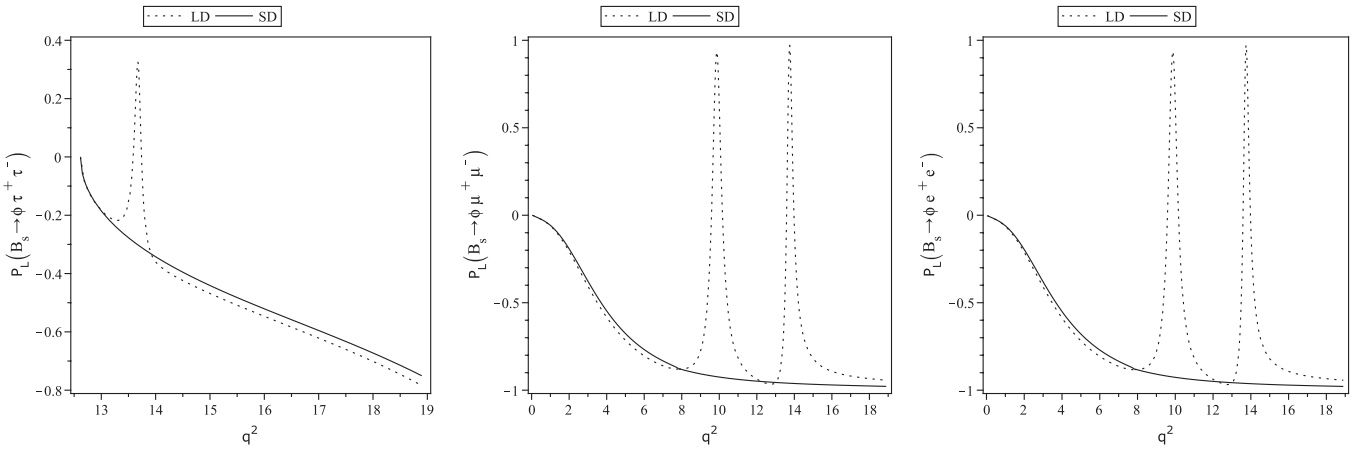


FIG. 6. The dependence of the longitudinal lepton polarization asymmetry on $q^2$. The solid lines and dotted lines show the results without and with the LD effects, respectively.

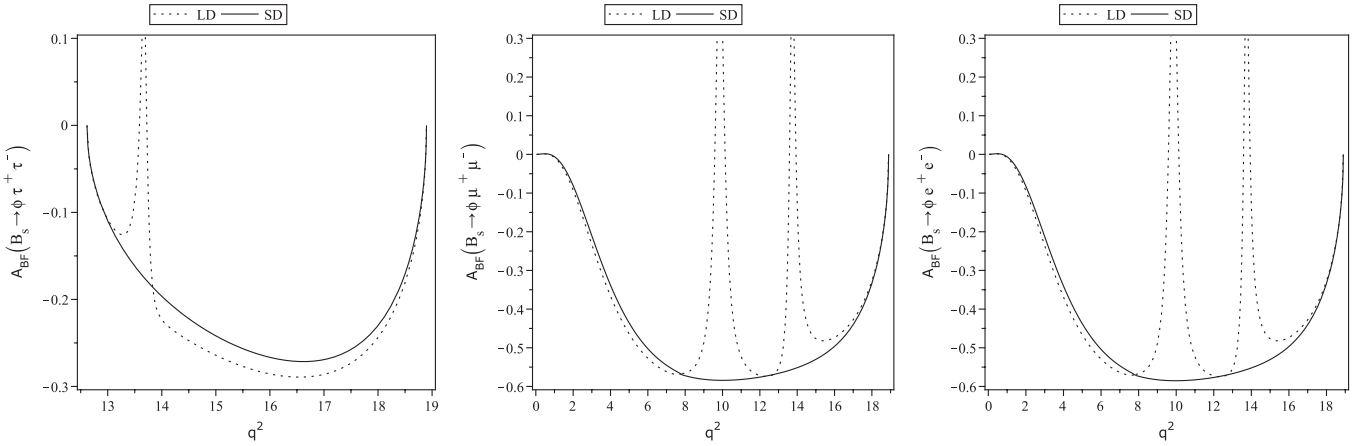


FIG. 7. The dependence of the forward-backward asymmetry on $q^2$. The solid lines and dotted lines show the results without and with the LD effects, respectively.

asymmetry for considered decays. They are given, respectively, as [10]

$$P_L = \frac{2(1-\frac{4t}{s})^{\frac{1}{2}}}{(1+\frac{2t}{s})\alpha_\phi + t\delta_\phi} \mathrm{Re}\Big\{\frac{1}{r_\phi}[\lambda_\phi^2 G_A^+ F_A^{+*} + \lambda_\phi(1-r_\phi) \times (1-r_\phi-s)(G_A^0 F_A^{+*} + G_A^+ F_A^{0*}) + (\lambda_\phi + 12 r_\phi s)(1-r_\phi)^2 G_A^0 F_A^{0*} + 8\lambda_\phi r_\phi s G_V F_V^*]\Big\},$$
$$A_{FB} = \frac{12 s \lambda_\phi^{\frac{1}{2}}(1-\frac{4t}{s})^{\frac{1}{2}}(1-r_\phi)\mathrm{Re}(G_V F_A^{0*} + G_A^0 F_V^*)}{(1+\frac{2t}{s})\alpha_\phi + t\delta_\phi}, \quad (28)$$

with all parameters and functions appearing in these formulas as defined before in Sec. II.

The dependences of the longitudinal lepton polarization and the forward-backward asymmetries for the $B_s \to \phi l^+ l^-$ decays on the transferred momentum square $q^2$ with and without LD effects are plotted in Figs. 6 and 7, respectively.

In summary, the transition form factors and the branching ratios of the semileptonic $B_s \to \phi$ decays as well as the longitudinal lepton polarization and forward-backward asymmetries were investigated. Any experimental measurements on the presented quantities and their comparison with the obtained results can give valuable information about the $B_s \to \phi l^+ l^- / \nu\bar{\nu}$ decays and the strong interactions inside them.

## ACKNOWLEDGMENTS

Partial support of the Isfahan University of Technology research council is appreciated.

## APPENDIX

In this appendix, the explicit expressions of the coefficients of the quark condensate entering the sum rules of the form factors $A_i$ ($i = V$, 0, 1, 2) and $T_j$ ($j = V$), 0, 1 are given.

$$
\begin{aligned}
C_0^A = {} & 2\frac{q^4 m_0^2}{M_1^4 M_2^4} - 6\frac{q^4 m_s^2}{M_1^4 M_2^4} + 2\frac{q^2 m_0^2}{M_1^2 M_2^4} - 3\frac{q^2 m_0^2 m_s^2}{M_1^2 M_2^6} + 6\frac{q^2 m_s^4}{M_1^2 M_2^6} - 2\frac{q^2 m_0^2}{M_1^4 M_2^2} + 6\frac{q^2 m_b m_s}{M_1^4 M_2^2} - 6\frac{q^2 m_s^2}{M_1^4 M_2^2} \\
& - 4\frac{q^2 m_0^2 m_b^2}{M_1^4 M_2^4} - 6\frac{q^2 m_0^2 m_b m_s}{M_1^4 M_2^4} - 4\frac{q^2 m_0^2 m_s^2}{M_1^4 M_2^4} + 12\frac{q^2 m_b^2 m_s^2}{M_1^4 M_2^4} + 12\frac{q^2 m_b m_s^3}{M_1^4 M_2^4} + 12\frac{q^2 m_s^4}{M_1^4 M_2^4} - 3\frac{q^2 m_0^2 m_b^2}{M_1^6 M_2^2} \\
& + 6\frac{q^2 m_b^2 m_s^2}{M_1^6 M_2^2} + \frac{m_0^2}{M_1^2 M_2^2} + 6\frac{m_b m_s}{M_1^2 M_2^2} - 6\frac{m_s^2}{M_1^2 M_2^2} - 2\frac{m_0^2 m_b^2}{M_1^2 M_2^4} - 6\frac{m_0^2 m_b m_s}{M_1^2 M_2^4} + 3\frac{m_0^2 m_b^2 m_s^2}{M_1^2 M_2^6} + 6\frac{m_0^2 m_b m_s^3}{M_1^2 M_2^6} \\
& + 3\frac{m_0^2 m_s^4}{M_1^2 M_2^6} - 6\frac{m_b^2 m_s^4}{M_1^2 M_2^6} - 12\frac{m_b m_s^5}{M_1^2 M_2^6} - 6\frac{m_s^6}{M_1^2 M_2^6} + 6\frac{m_0^2 m_b m_s}{M_1^4 M_2^2} + 2\frac{m_0^2 m_s^2}{M_1^4 M_2^2} - 6\frac{m_b^3 m_s}{M_1^4 M_2^2} - 6\frac{m_b^2 m_s^2}{M_1^4 M_2^2} \\
& + 6\frac{m_b m_s^3}{M_1^4 M_2^2} + 6\frac{m_s^4}{M_1^4 M_2^2} + 2\frac{m_0^2 m_b^4}{M_1^4 M_2^4} + 6\frac{m_0^2 m_b^3 m_s}{M_1^4 M_2^4} + 8\frac{m_0^2 m_b^2 m_s^2}{M_1^4 M_2^4} + 6\frac{m_0^2 m_b m_s^3}{M_1^4 M_2^4} + 2\frac{m_0^2 m_s^4}{M_1^4 M_2^4} - 6\frac{m_b^4 m_s^2}{M_1^4 M_2^4} \\
& - 12\frac{m_b^3 m_s^3}{M_1^4 M_2^4} - 12\frac{m_b^2 m_s^4}{M_1^4 M_2^4} - 12\frac{m_b m_s^5}{M_1^4 M_2^4} - 6\frac{m_s^6}{M_1^4 M_2^4} + 3\frac{m_0^2 m_b^4}{M_1^6 M_2^2} + 6\frac{m_0^2 m_b^3 m_s}{M_1^6 M_2^2} + 3\frac{m_0^2 m_b^2 m_s^2}{M_1^6 M_2^2} - 6\frac{m_b^4 m_s^2}{M_1^6 M_2^2} \\
& - 12\frac{m_b^3 m_s^3}{M_1^6 M_2^2} - 6\frac{m_b^2 m_s^4}{M_1^6 M_2^2}.
\end{aligned}
$$

$$
\begin{aligned}
C_V^A = {} & 4\frac{q^2 m_0^2}{M_1^4 M_2^4} - 12\frac{q^2 m_s^2}{M_1^4 M_2^4} + 12\frac{m_s^2}{M_1^2 M_2^4} - 6\frac{m_0^2 m_s^2}{M_1^2 M_2^6} + 12\frac{m_s^4}{M_1^2 M_2^6} - 8\frac{m_0^2}{M_1^4 M_2^2} + 12\frac{m_b m_s}{M_1^4 M_2^2} - 4\frac{m_0^2 m_b^2}{M_1^4 M_2^4} \\
& - 4\frac{m_0^2 m_b m_s}{M_1^4 M_2^4} - 4\frac{m_0^2 m_s^2}{M_1^4 M_2^4} + 12\frac{m_b^2 m_s^2}{M_1^4 M_2^4} + 12\frac{m_s^4}{M_1^4 M_2^4} - 6\frac{m_0^2 m_b^2}{M_1^6 M_2^2} + 12\frac{m_b^2 m_s^2}{M_1^6 M_2^2}.
\end{aligned}
$$

$$
\begin{aligned}
C_1^A = {} & 4\frac{q^2 m_0^2}{M_1^4 M_2^4} - 12\frac{q^2 m_s^2}{M_1^4 M_2^4} + 12\frac{m_s^2}{M_1^2 M_2^4} - 6\frac{m_0^2 m_s^2}{M_1^2 M_2^6} + 12\frac{m_s^4}{M_1^2 M_2^6} - 16\frac{m_0^2}{M_1^4 M_2^2} + 12\frac{m_b m_s}{M_1^4 M_2^2} + 24\frac{m_s^2}{M_1^4 M_2^2} \\
& - 4\frac{m_0^2 m_b^2}{M_1^4 M_2^4} - 4\frac{m_0^2 m_b m_s}{M_1^4 M_2^4} - 4\frac{m_0^2 m_s^2}{M_1^4 M_2^4} + 12\frac{m_b^2 m_s^2}{M_1^4 M_2^4} + 12\frac{m_s^4}{M_1^4 M_2^4} - 6\frac{m_0^2 m_b^2}{M_1^6 M_2^2} + 12\frac{m_b^2 m_s^2}{M_1^6 M_2^2}.
\end{aligned}
$$

$$
\begin{aligned}
C_2^A = {} & -4\frac{q^2 m_0^2}{M_1^4 M_2^4} + 12\frac{q^2 m_s^2}{M_1^4 M_2^4} - 12\frac{m_s^2}{M_1^2 M_2^4} + 6\frac{m_0^2 m_s^2}{M_1^2 M_2^6} - 12\frac{m_s^4}{M_1^2 M_2^6} - 12\frac{m_b m_s}{M_1^4 M_2^2} + 24\frac{m_s^2}{M_1^4 M_2^2} + 4\frac{m_0^2 m_b^2}{M_1^4 M_2^4} \\
& + 4\frac{m_0^2 m_b m_s}{M_1^4 M_2^4} + 4\frac{m_0^2 m_s^2}{M_1^4 M_2^4} - 12\frac{m_b^2 m_s^2}{M_1^4 M_2^4} - 12\frac{m_s^4}{M_1^4 M_2^4}. + 6\frac{m_0^2 m_b^2}{M_1^6 M_2^2} - 12\frac{m_b^2 m_s^2}{M_1^6 M_2^2}.
\end{aligned}
$$

$$
\begin{aligned}
C_0^T = {} & -2\frac{q^4 m_0^2 m_b}{M_1^4 M_2^4} + 2\frac{q^4 m_0^2 m_s}{M_1^4 M_2^4} + 6\frac{q^4 m_b m_s^2}{M_1^4 M_2^4} - 6\frac{q^4 m_s^3}{M_1^4 M_2^4} - \frac{q^2 m_0^2 m_b}{M_1^2 M_2^4} + 3\frac{q^2 m_0^2 m_s}{M_1^2 M_2^4} + 3\frac{q^2 m_0^2 m_b m_s^2}{M_1^2 M_2^6} - 3\frac{q^2 m_0^2 m_s^3}{M_1^2 M_2^6} \\
& - 6\frac{q^2 m_b m_s^4}{M_1^2 M_2^6} + 6\frac{q^2 m_s^5}{M_1^2 M_2^6} - 2\frac{q^2 m_0^2 m_b}{M_1^4 M_2^2} - 2\frac{q^2 m_0^2 m_s}{M_1^4 M_2^2} + 6\frac{q^2 m_b m_s^2}{M_1^4 M_2^2} + 4\frac{q^2 m_0^2 m_b^3}{M_1^4 M_2^4} + \frac{q^2 m_0^2 m_b^2 m_s}{M_1^4 M_2^4} \\
& - \frac{q^2 m_0^2 m_b m_s^2}{M_1^4 M_2^4} - 4\frac{q^2 m_0^2 m_s^3}{M_1^4 M_2^4} - 12\frac{q^2 m_b^3 m_s^2}{M_1^4 M_2^4} + 12\frac{q^2 m_s^5}{M_1^4 M_2^4} + 3\frac{q^2 m_0^2 m_b^3}{M_1^6 M_2^2} - 3\frac{q^2 m_0^2 m_b^2 m_s}{M_1^6 M_2^2} - 6\frac{q^2 m_b^3 m_s^2}{M_1^6 M_2^2} \\
& + 6\frac{q^2 m_b^2 m_s^3}{M_1^6 M_2^2} - \frac{m_0^2 m_b}{M_1^2 M_2^2} + 6\frac{m_b m_s^2}{M_1^2 M_2^2} + 6\frac{m_s^3}{M_1^2 M_2^2} + \frac{m_0^2 m_b^3}{M_1^2 M_2^4} + 2\frac{m_0^2 m_b^2 m_s}{M_1^2 M_2^4} - 2\frac{m_0^2 m_b m_s^2}{M_1^2 M_2^4} - 3\frac{m_0^2 m_s^3}{M_1^2 M_2^4} \\
& - 3\frac{m_0^2 m_b^3 m_s^2}{M_1^2 M_2^6} - 3\frac{m_0^2 m_b^2 m_s^3}{M_1^2 M_2^6} + 3\frac{m_0^2 m_b m_s^4}{M_1^2 M_2^6} + 3\frac{m_0^2 m_s^5}{M_1^2 M_2^6} + 6\frac{m_b^3 m_s^4}{M_1^2 M_2^6} + 6\frac{m_b^2 m_s^5}{M_1^2 M_2^6} - 6\frac{m_b m_s^6}{M_1^2 M_2^6} - 6\frac{m_s^7}{M_1^2 M_2^6}
\end{aligned}
$$

$$+4\frac{m_0^2 m_b^3}{M_1^4 M_2^2}+2\frac{m_0^2 m_b^2 m_s}{M_1^4 M_2^2}-3\frac{m_0^2 m_b m_s^2}{M_1^4 M_2^2}-\frac{m_0^2 m_s^3}{M_1^4 M_2^2}-6\frac{m_b^3 m_s^2}{M_1^4 M_2^2}-6\frac{m_b^2 m_s^3}{M_1^4 M_2^2}+6\frac{m_b m_s^4}{M_1^4 M_2^2}+6\frac{m_s^5}{M_1^4 M_2^2}$$
$$-2\frac{m_0^2 m_b^5}{M_1^4 M_2^4}-3\frac{m_0^2 m_b^4 m_s}{M_1^4 M_2^4}-\frac{m_0^2 m_b^3 m_s^2}{M_1^4 M_2^4}+\frac{m_0^2 m_b^2 m_s^3}{M_1^4 M_2^4}+3\frac{m_0^2 m_b m_s^4}{M_1^4 M_2^4}+2\frac{m_0^2 m_s^5}{M_1^4 M_2^4}+6\frac{m_b^5 m_s^2}{M_1^4 M_2^4}+6\frac{m_b^4 m_s^3}{M_1^4 M_2^4}$$
$$-6\frac{m_b m_s^6}{M_1^4 M_2^4}-6\frac{m_s^7}{M_1^4 M_2^4}-3\frac{m_0^2 m_b^5}{M_1^6 M_2^2}-3\frac{m_0^2 m_b^4 m_s}{M_1^6 M_2^2}+3\frac{m_0^2 m_b^3 m_s^2}{M_1^6 M_2^2}+3\frac{m_0^2 m_b^2 m_s^3}{M_1^6 M_2^2}+6\frac{m_b^5 m_s^2}{M_1^6 M_2^2}+6\frac{m_b^4 m_s^3}{M_1^6 M_2^2}$$
$$-6\frac{m_b^3 m_s^4}{M_1^6 M_2^2}-6\frac{m_b^2 m_s^5}{M_1^6 M_2^2}+6\frac{m_0^2 m_s}{M_1^4 M_2^2}.$$

$$C_V^T=4\frac{q^2 m_0^2 m_b}{M_1^4 M_2^4}+4\frac{q^2 m_0^2 m_s}{M_1^4 M_2^4}-12\frac{q^2 m_b m_s^2}{M_1^4 M_2^4}-12\frac{q^2 m_s^3}{M_1^4 M_2^4}-2\frac{m_0^2 m_b}{M_1^2 M_2^4}-2\frac{m_0^2 m_s}{M_1^2 M_2^4}+12\frac{m_b m_s^2}{M_1^2 M_2^4}+12\frac{m_s^3}{M_1^2 M_2^4}$$
$$-6\frac{m_0^2 m_b m_s^2}{M_1^2 M_2^6}-6\frac{m_0^2 m_s^3}{M_1^2 M_2^6}+12\frac{m_b m_s^4}{M_1^2 M_2^6}+12\frac{m_s^5}{M_1^2 M_2^6}-12\frac{m_0^2 m_b}{M_1^4 M_2^2}-8\frac{m_0^2 m_s}{M_1^4 M_2^2}-4\frac{m_0^2 m_b^3}{M_1^4 M_2^4}-6\frac{m_0^2 m_b^2 m_s}{M_1^4 M_2^4}$$
$$-6\frac{m_0^2 m_b m_s^2}{M_1^4 M_2^4}-4\frac{m_0^2 m_s^3}{M_1^4 M_2^4}+12\frac{m_b^3 m_s^2}{M_1^4 M_2^4}+12\frac{m_b^2 m_s^3}{M_1^4 M_2^4}+12\frac{m_b m_s^4}{M_1^4 M_2^4}+12\frac{m_s^5}{M_1^4 M_2^4}-6\frac{m_0^2 m_b^3}{M_1^6 M_2^2}-6\frac{m_0^2 m_b^2 m_s}{M_1^6 M_2^2}$$
$$+12\frac{m_b^3 m_s^2}{M_1^6 M_2^2}+12\frac{m_b^2 m_s^3}{M_1^6 M_2^2}.$$

$$C_1^T=6\frac{q^2 m_0^2 m_b}{M_1^4 M_2^4}-4\frac{q^2 m_0^2 m_s}{M_1^4 M_2^4}-12\frac{q^2 m_b m_s^2}{M_1^4 M_2^4}+12\frac{q^2 m_s^3}{M_1^4 M_2^4}-10\frac{m_0^2 m_s}{M_1^2 M_2^4}+12\frac{m_b m_s^2}{M_1^2 M_2^4}+12\frac{m_s^3}{M_1^2 M_2^4}-6\frac{m_0^2 m_b m_s^2}{M_1^2 M_2^6}$$
$$+6\frac{m_0^2 m_s^3}{M_1^2 M_2^6}+12\frac{m_b m_s^4}{M_1^2 M_2^6}-12\frac{m_s^5}{M_1^2 M_2^6}-14\frac{m_0^2 m_b}{M_1^4 M_2^2}+8\frac{m_0^2 m_s}{M_1^4 M_2^2}-24\frac{m_b m_s^2}{M_1^4 M_2^2}-6\frac{m_0^2 m_b^3}{M_1^4 M_2^4}+4\frac{m_0^2 m_b^2 m_s}{M_1^4 M_2^4}$$
$$-4\frac{m_0^2 m_b m_s^2}{M_1^4 M_2^4}+4\frac{m_0^2 m_s^3}{M_1^4 M_2^4}+12\frac{m_b^3 m_s^2}{M_1^4 M_2^4}-12\frac{m_b^2 m_s^3}{M_1^4 M_2^4}+12\frac{m_b m_s^4}{M_1^4 M_2^4}-12\frac{m_s^5}{M_1^4 M_2^4}-6\frac{m_0^2 m_b^3}{M_1^6 M_2^2}+6\frac{m_0^2 m_b^2 m_s}{M_1^6 M_2^2}$$
$$+12\frac{m_b^3 m_s^2}{M_1^6 M_2^2}-12\frac{m_b^2 m_s^3}{M_1^6 M_2^2}.$$


[1] M. Artuso, E. Barberio, and S. Stone, PMC Phys. A **3**, 3 (2009).
[2] C. S. Kim, T. Morozumi, and A. I. Sanda, Phys. Rev. D **56**, 7240 (1997); A. Ali and G. Hiller, Eur. Phys. J. C **8**, 619 (1999).
[3] N. Ghahramany and R. Khosravi, Phys. Rev. D **80**, 016009 (2009).
[4] A. Deandrea and A. D. Polosa, Phys. Rev. D **64**, 074012 (2001).
[5] J. L. Hewett, in *Proceedings of the 21st Annual SLAC Summer Institute*, edited by L. DePorcel and C. Dunwoodie (SLAC-Report-444, Stanford, CA, 1994).
[6] G. Erkol and G. Turan, Eur. Phys. J. C **25**, 575 (2002).
[7] J. M. Flynn and C. T. Sachrajda, Adv. Ser. Dir. High Energy Phys. **15**, 402 (1998).
[8] P. Ball and V. M. Braun, Phys. Rev. D **58**, 094016 (1998).
[9] D. Melikhov and B. Stech, Phys. Rev. D **62**, 014006 (2000).
[10] C. Q. Geng and C. C. Liu, J. Phys. G **29**, 1103 (2003).
[11] C. Q. Geng, C. W. Hwang, C. C. Lih, and W. M. Zhang, Phys. Rev. D **64**, 114024 (2001).
[12] H. Y. Cheng, C. Y. Cheung, and C. W. Hwang, Phys. Rev. D **55**, 1559 (1997).
[13] P. Colangelo and A. Khodjamirian, in *At the Frontier of Particle Physics/Handbook of QCD*, edited by M. Shifman (World Scientific, Singapore, 2001), Vol. III, p. 1495.
[14] R. Khosravi and M. Janbazi, Phys. Rev. D **87**, 016003 (2013).
[15] M. A. Shifman, A. I. Vainshtein, and V. I. Zakharov, Nucl. Phys. **B147**, 385 (1979); **B147**, 448 (1979).
[16] K. C. Bowler *et al.* (UKQCD Collaboration), Phys. Rev. D **52**, 5067 (1995).
[17] J. Beringer *et al.* (Particle Data Group), Phys. Rev. D **86**, 010001 (2012).
[18] P. Ball and R. Zwicky, Phys. Rev. D **71**, 014029 (2005).
[19] A. Faessler, Th. Gutsche, M. A. Ivanov, J. G. Korner, and V. E. Lyubovitskij, Eur. Phys. J. C **4**, 18 (2002).
[20] I. Bediaga and M. Nielsen, Phys. Rev. D **68**, 036001 (2003).
[21] A. J. Buras and M. Muenz, Phys. Rev. D **52**, 186 (1995).